IEEE Access
Multidisciplinary | Rapid Review | Open Access Journal

Received May 1, 2018, accepted May 19, 2018, date of publication May 30, 2018, date of current version June 19, 2018.

Digital Object Identifier 10.1109/ACCESS.2018.2840333

Numerical Investigation of the Dynamic Responses of Long-Span Bridges With Consideration of the Random Traffic Flow Based on the Intelligent ACO-BPNN Model

LIWEN ZHANG[1], ZHUO SUN[1], CHAO ZHANG[1], FENGHUI DONG[2], AND PU WEI[3]

[1]Department of Civil Engineering, Guangzhou University, Guangzhou 510006, China
[2]Department of Bridge Engineering, College of Civil Engineering, Tongji University, Shanghai 200092, China
[3]Shanghai Municipal Engineering Design Institute, Shanghai 200092, China

Corresponding author: Zhuo Sun (szhuogz@163.com)

This work was supported by the National Natural Science Foundation of China under Grant 51608137.

ABSTRACT With emphasis on long-span bridges, the dynamic responses of bridges without considering random traffic flows were found to be different from actual situations. The introduction of a random traffic flow model provides a new approach for the random analysis of bridge structure responses under vehicle loads. In this paper, the finite element and intelligent ant colony optimization-back propagation neural network (ACO-BPNN) models were used to study the dynamic responses of long-span bridges. The computational model was also validated by an experimental test. To confirm the validity of the proposed ACO-BPNN model after parameter selection, it was compared with the traditional back propagation neural network (BPNN) model and the genetic algorithm-back propagation neural network (GA-BPNN) model. BPNN, GA-BPNN, and ACO-BPNN adopt the same network topology structure to predict the dynamic responses of the long-span bridge. When the ACO-BPNN model conducted the iteration to the 130th generation, a training error of 0.009 was found to be smaller than the set critical error. In this manner, the computational accuracy was increased, and the optimized time was reduced. In addition, only 0.4 hours were spent in using the proposed ACO-BPNN model to predict the dynamic response of the long-span bridge. In the case of the same computer performance, it took 4.5 h to use the finite element model to predict the dynamic response of the long-span bridge. The advantage of the proposed ACO-BPNN model in predicting the performance of large-scale complex structures such as long-span bridges was clearly found.

INDEX TERMS Dynamic responses, long-span bridges, random traffic flow, ACO-BPNN model, finite element model.

I. INTRODUCTION

Traffic and transportation are becoming increasingly important with continued social development and the enhancement of economic complementarity and interdependency, with bridges playing a key role. While passing traffic obstacles, including great rivers, high mountains, gorges and harbor ports, a long-span bridge is always the preferred bridge type because of its superiority in structural force bearing [1]–[5]. General long-span bridges crossing rivers have very large spans. It is very important to study their responses under various loads to ensure their safe and reliable operation. With the increase in vehicle running speed, the dynamic interaction problem between vehicles and a bridge becomes more prominent, and the impacts of vehicle-bridge coupling dynamic interactions on the bridge and vehicles become increasingly obvious. Vehicles run at very high speeds, and vehicle actions are always amplified under the effects of road roughness, thereby seriously affecting bridge safety. Therefore, it is increasingly meaningful to study dynamic problems between vehicles and bridges. On one hand, dynamic impacts of movable vehicles on a structure could have direct effects on working conditions and the service life of

the structure; on the other hand, the steadiness and the safety of vehicles running on the structure are also important factors to assess whether dynamic design parameters of the structure are rational. At present, new bridges always have large spans, requiring the use of many high-strength materials and thin-walled structures. The bridge span becomes increasingly larger, materials become increasingly lighter, and rigidity becomes increasingly lower; as a result, the proportion occupied by loads borne by the bridge structure in total loads becomes increasingly larger, thereby intensifying interactions between vehicles and bridges.

At present, abundant achievements have been achieved in studies on vehicle-bridge coupling vibration [6]–[11]. Ding *et al.* [12] applied the d'Alembert principle and displacement coordination conditions to deduce a motion equation of vehicle-bridge coupling vibration and discussed the impacts of a single vehicle load on the vibration responses of a long-span bridge with consideration of geometric nonlinearity and deck roughness factors. Pang *et al.* [13] applied state space theories to establish a finite element model of vehicle-bridge coupling vibration and studied the vehicle-bridge coupling vibration problem of a long-span bridge under movable vehicles. Xiao and Ren [14] conducted an analysis and computations of vehicle-bridge coupling vibrations under various working conditions, analyzed and evaluated the dynamic responses of bridges and vehicles, as well as the running safety and steadiness, obtaining some conclusions with engineering significance. Aiming at numerical analysis of the vehicle-bridge coupling vibration of a complicated bridge, Shi *et al.* [15] proposed a method for computing the vehicle-bridge coupling vibration of complicated bridges on highways using the finite element software ANSYS. Ye *et al.* [16] took the deck roughness power spectral density as the input to establish a vehicle-bridge coupling dynamic analysis model and discussed the impacts of mid-span support, flexural rigidity of bridge cross section, running speed and deck roughness on random responses of a vehicle-bridge coupling system. Zhang *et al.* [17] used the finite element software MIDAS to analyze the dynamic characteristics of a bridge under different factors and studied the changing rules of indices, including mid-span displacement, bending moment impact coefficient and acceleration. Based on random vibration theories, Zhang *et al.* [18] studied a bridge dynamic response curve with vehicle-bridge coupling vibration under the effects of deterministic excitation and deck roughness. Taking the unevenness power spectrum density function of the surface of a deck structure as the input, Ye *et al.* [19] established a coupled dynamic analysis model with multiple movable vehicle systems and a bridge and discussed the changing rules of mid-span displacement under different spans, different deck grades and different vehicle speeds.

However, the aforementioned studies are based on deterministic analysis, which cannot reflect the random characteristics of bridge responses. Aiming at long-span bridges, the dynamic responses of bridges without considering random traffic flows were found to be different from actual situations [20]–[23].

In this paper, section 2 described the establishment of the finite element model, section 3 analyzed and discussed the dynamic response of the long-span bridge, and section 4 has predicted the dynamic response using the intelligent ACO-BPNN (Ant Colony Optimization-Back Propagation Neural Network) models, laying a foundation for dynamic response analysis of bridges under random traffic flows.

II. ESTABLISHMENT OF THE FINITE ELEMENT MODEL OF LONG-SPAN BRIDGES

Fig. 1 shows a long-span bridge with a simple support, where the bridge span is arranged as a single span of 200 m, with the total bridge length of 800 m; the center distance of the main cable of 6 m, the width of the traffic lane is 4.5 m, and the width of the long-span bridge is 35 m; the cable tower has an inverse-Y structure made of solid reinforced concrete. For convenience of modeling, the height of both the left and right cable towers is 30 m. A geometric model of the long-span bridge was established according to the dimensions and layout, as shown in Fig. 2.

In this paper, the finite element software ANSYS was used for computation. In the ANSYS model, the cross section of the cable tower was variable; thus, BEAM44 elements, namely, spatial cross-section-variable beam elements, were used. The main beam adopted a traditional single-beam form. The cross section of the main beam was basically deemed to be unchanged along the bridge direction. BEAM4 spatial beam elements were used. A rigid arm connection method was used during modeling in the paper. Each node of the element only has three degrees of freedom. Gravity rigidity of the long-span bridge had obvious impacts on changes of structural rigidity. Finally, the complete bridge was divided into 5949 nodes and 10040 elements. The complete finite element model of the long-span bridge is shown in Fig. 2.

The connection of the different structures was achieved as follows. The CP command of the nodes in ANSYS was used to couple three translational degrees of freedom and three rotational degrees of freedom between two nodes. The cable towers and piers were completely solidified, and the degrees of freedom in 6 directions were constrained. The material property of the long-span bridge is as follows: the elastic modulus of main towers is $3.65e^{10}$ N/m^2, the density of main towers is 2600 kg/m^3, the elastic modulus of main beams is $4.0e^{10}$ N/m^2, the density of main beams is 2600 kg/m^3, the elastic modulus of cables is $1.95e^{11}$ N/m^2, and the density of cables is 7850 kg/m^3. Finally, the vibration shapes at the top 10 orders of the long-span bridge could be computed. The frequencies of each order of vibration shapes were 0.51 Hz, 0.67 Hz, 0.76 Hz, 0.85 Hz, 0.96 Hz, 1.06 Hz, 1.12 Hz, 1.21 Hz, 1.34 Hz and 1.56 Hz. Clearly, the frequency distribution was very dense and could satisfy the dense distribution characteristic of natural frequencies of large infrastructures. Some of the vibration shapes extracted are shown in Fig. 3. In addition, the figure shows that the

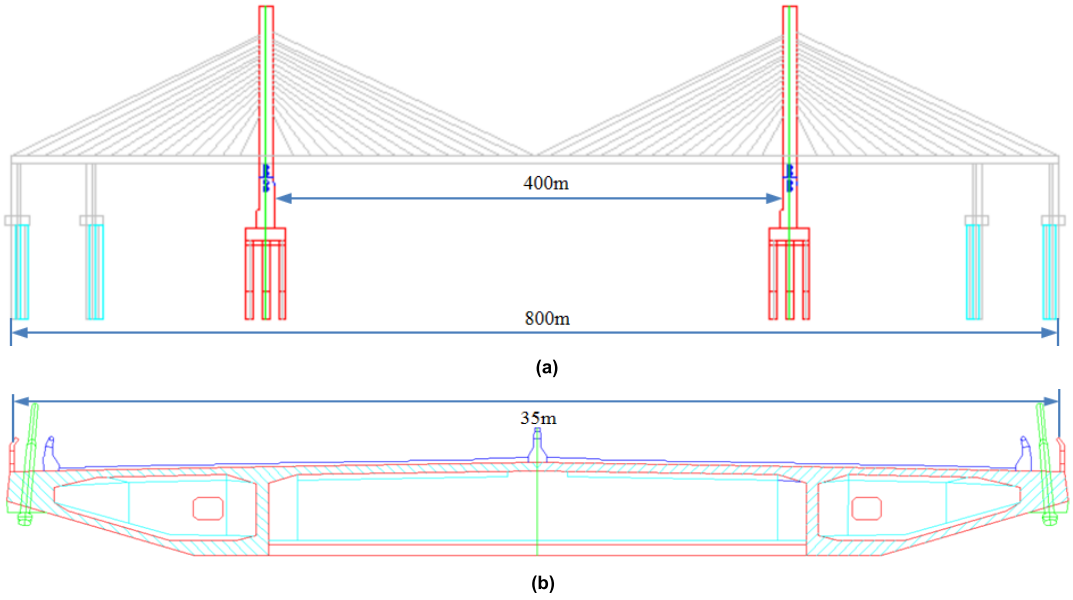

FIGURE 1. Two-dimensional model and dimensions of a long-span bridge. (a) Complete model. (b) Box girder model.

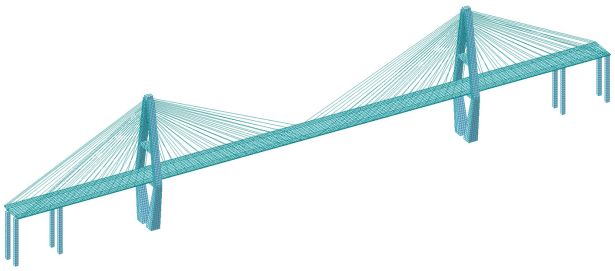

FIGURE 2. Complete finite element model of the long-span bridge.

first-order vibration shape was mainly reflected by bending vibration of cable towers and piers. The second-order vibration shape was reflected by the first-order bending vibration of the box girder. The third-order vibration shape was reflected by the second-order bending vibration of the box girder. The fourth-order vibration mode was reflected by the torsional vibration of the box girder. The fifth-order vibration shape was reflected by bending and torsional coupling vibration of the box girder. The vibration shapes were mainly reflected by bending and torsional vibration of the box girder and the cable towers. Therefore, the vibration shapes of the long-span bridge were not purely torsional or bending vibration; sometimes, they referred to overlaying of the two types of vibration.

III. ANALYSIS AND DISCUSSION OF THE DYNAMIC RESPONSES OF LONG-SPAN BRIDGES

A. NUMERICAL COMPUTATION OF THE BRIDGE DYNAMIC RESPONSES UNDER RANDOM TRAFFIC FLOW

A time-domain model of vehicles was established. In the model, random traffic flows are generated in the time domain according to the following steps. First, the vehicle running flow rate is monitored based on WIM (dynamic weighing system), and a random vehicle flow database is established; Monte Carlo sampling is used on the MATLAB platform to generate random traffic flow samples. The random vehicles mainly have 4 random parameters: vehicle type, vehicle speed, mass and vehicle distance. The vehicle types generally obey a uniform distribution. The studied results of [24] showed that the vehicle distances obey a Gamma distribution. Highway bridge vehicles have very high randomness and basically satisfy the characteristic of high randomness of the MATLAB program. By virtue of the advantage that the program can call various random functions and could randomly generate various types of data samples according to the requirements, in this paper, a simulation program of random traffic flows was compiled. Next, a random traffic flow document was generated and input into the vehicle-bridge coupling analysis program to study the bridge dynamic responses. The specific steps are as follows. First, a random traffic flow document was generated; the vehicle distances were converted into a finite element node matrix of the bridge, and the vehicle loading positions were recognized according to the vehicle distances. Conversion of the vehicle distances into bridge node matrices is a key step. The vehicle distances were added to determine the position matrix of each vehicle in the traffic flow, and then, the position matrices were converted into node matrices according to vehicle speeds; with an increase of the transient analysis step length, the node matrix of the vehicle was checked to determine whether an initial bridge node was reached, and whether the front vehicles already passed the bridge was recognized. The vehicles were loaded or canceled, and thus, transient analysis could be conducted.

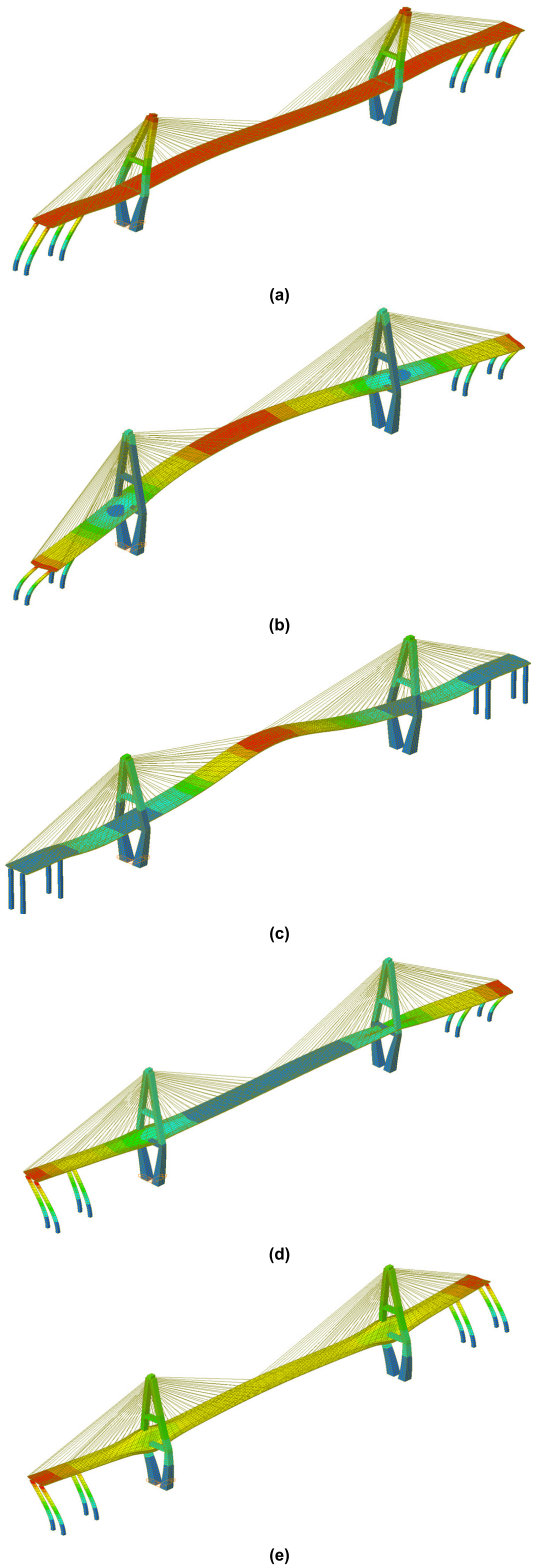

FIGURE 3. Natural vibration shapes of the long-span bridge. (a) First order vibration shape. (b) Second order vibration shape. (c) Third order vibration shape. (d) Fourth order vibration shape. (e) Fifth order vibration shape.

As mentioned, through combining ANSYS with MATLAB, co-simulation was conducted and bridge dynamic responses under the random traffic flow were obtained. Fig. 4 and Fig. 5 show vibration displacement and acceleration response curves of the bridge, respectively. It is shown in the figure that the responses at different positions of the long-span bridge were different. (1) The results of vibration displacement and acceleration of the bridge fluctuated around 0. (2) The displacement response peak at the L/4 position of the long-span bridge was −80 mm. (3) The displacement response peak at the L/2 position of the long-span bridge was −70 mm, and the displacement response peak value at the L/4 position was approximately 1.14 times compared with the displacement response peak at the L/2 position. (4) The displacement response mean at the L/4 position of the long-span bridge was 25 mm; the response means at the position of L/2 was 33 mm; the response means at the position of L/4 was approximately 0.76 times compared with that of the position of L/2. The vibration displacement and acceleration of the bridge were large because the vehicle loads acting on the bridge were large. Vibration displacements and accelerations at the position of L/4 clearly exceeded those at the position of L/2 because new vehicles ran onto the bridge continuously. The L/4 position was first affected by these vehicle loads.

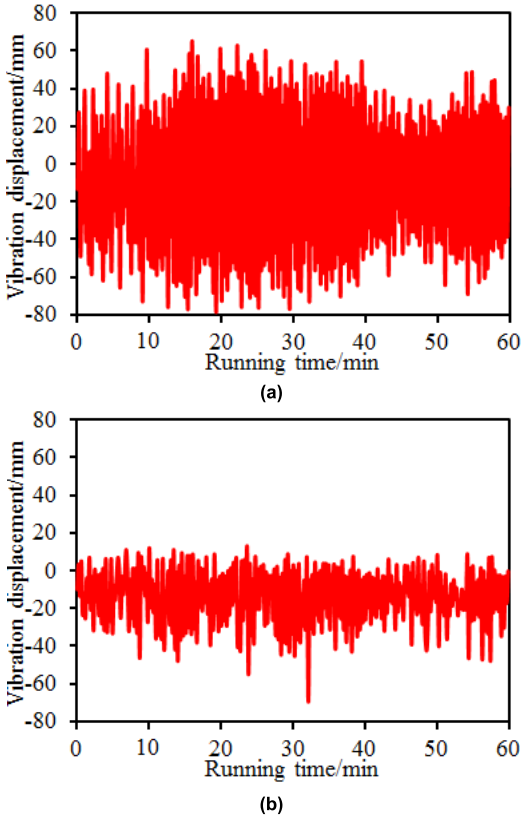

FIGURE 4. Vibration displacement of the long-span bridge. (a) Position = L/4. (b) Position = L/2.

B. EXPERIMENTAL VERIFICATION OF BRIDGE DYNAMIC RESPONSES

Such a complicated computation model of long-span bridges is affected by many parameters. Therefore, the correctness of the model should be verified by experimental tests.

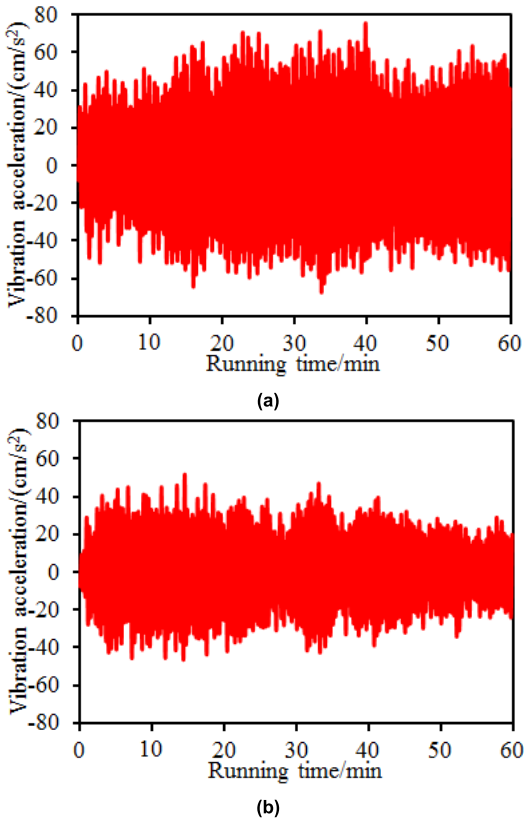

FIGURE 5. Vibration acceleration of the long-span bridge. (a) Position = L/4. (b) Position = L/2.

With numerical simulation as the reference, single-way servo acceleration sensors [25]–[30] with sampling frequency of 100 Hz were arranged, with a pair of sensors at each the positions of L/4, L/2 and 3L/4 of the long-span bridge, as shown in Fig. 6. Therefore, there were six sensors on the bridge, and the average value of each pair of sensors was that of the final results. When vehicles ran on the bridge normally, the data of the acceleration sensors was recorded and input into Pulse software for post-processing. Time-domain vibration displacement measurements were obtained and compared with the computational results of the numerical simulation, as shown in Fig. 7. Fig. 7 reveals that the experimental results were well consistent with the numerical simulation results. Under most cases, the experimental test results were slightly larger than the numerical simulation results; the numerical simulation considers an ideal boundary condition, whereas the experimental boundary conditions are relatively complicated. Therefore, complete consistency could not be achieved. In addition, the experimental results were also affected by crosswind. Numerical simulation could consider vehicle-bridge coupling. However, as a whole, the numerical simulation computation model proposed by the paper is reliable.

Experimental testing results showed that the numerical computation model proposed by the paper is reliable. Therefore, the root-mean-square values of vibration displacements at each position of the bridge were computed based on the numerical model, as shown in Fig. 8. The figure indicates that root-mean-square values of the bridge vibration displacement were basically symmetric relative to the mid-span position. Within 0-L/4, the root-mean-square values of vibration displacement sharply increased to the maximum value and then decreased slowly. The maximum root-mean-square values of the vibration displacement were approximately at the positions of L/4 and 3L/4 of the bridge. The valley values of the root-mean-square curve were located at the bridge mid-span position.

IV. DYNAMIC RESPONSE ANALYSIS ON BRIDGES BASED ON THE aco-bpnn METHOD

As mentioned, co-simulation was conducted on the vehicle-bridge coupling vibration responses based on ANSYS and MATLAB. However, the computation was too complicated, and the computational time was too long. Therefore, in this paper, an intelligent algorithm was used to compute dynamic responses of the bridge under random traffic flows. Neural network is a widely applied intelligent algorithm [31]–[37]. The topological structure is shown in Fig. 9. In this figure, the first layer is input layer, the second and third layers are hidden layer, the last layer is output layer. A multi-layer feed-forward neural network model (BPNN) is widely used in the neural network. BPNN has features of clear concepts and simple computation. Because of the rigorous derivation and high universality, BPNN is widely applied. However, the BPNN algorithm is essentially a local search algorithm and cannot be used to search global extremes of multi-peak functions. BPNN also has defects, such as long convergence time and easy appearance of local extremes. For these reasons, many improved algorithms have been proposed, with the BPNN algorithm with a momentum item being the simplest one that can be achieved easily. Nevertheless, BPNN is still a local search algorithm; therefore, essentially speaking, it still cannot get rid of the possibility of falling into local minimum points.

Once proposed, the Ant Colony Optimization (ACO) algorithm has become a popular topic of discussion and study in the field of intelligent optimization and evolutionary fields. Through many years of development, scholars have performed careful research studies on the ACO algorithm. The algorithm has obtained great improvements and is widely applied in fields such as the solution of cooperative problems, data analysis, water conservancy, electric power, construction and transportation. The ACO algorithm has drawn the attention of scholars in related fields because the solution model could rationally combine the rapidness of problem solution and global optimization characteristics. Thus, rapidness of optimization is ensured by forward-feedback information transmission and accumulation. Premature convergence of the algorithm could be avoided by the characteristic of distributed computation. Moreover, an ant colony system with a greedy heuristic search characteristic could find acceptable solutions at earlier stages of the search. Therefore, the paper

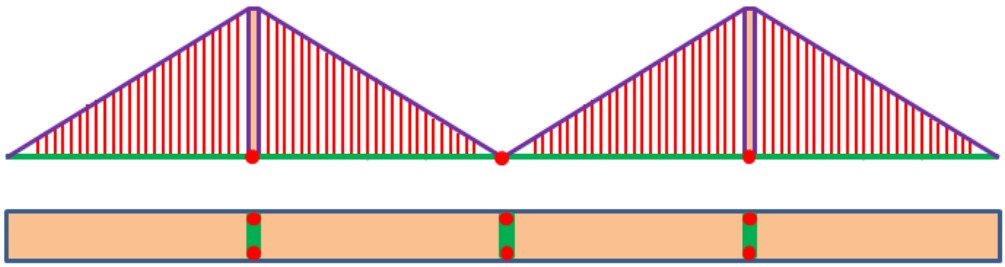

FIGURE 6. Experimental test of the vibration displacement of the long-span bridge.

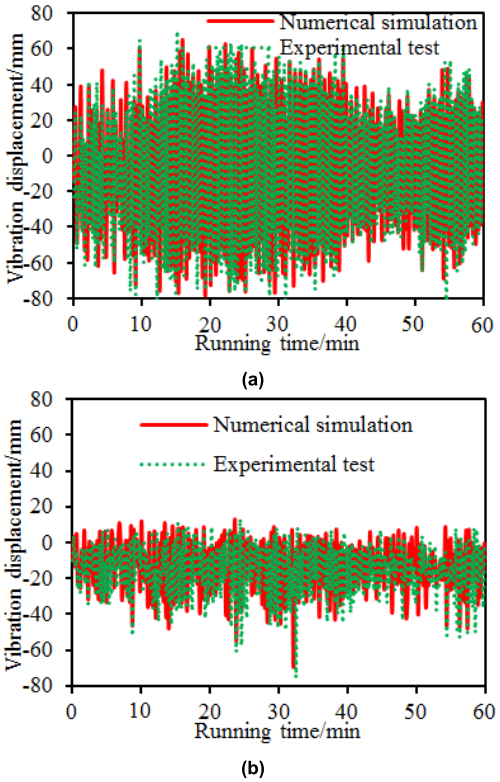

FIGURE 7. Experimental and simulation comparison of the vibration displacement of the long-span bridge. (a) Position = L/4. (b) Position = L/2.

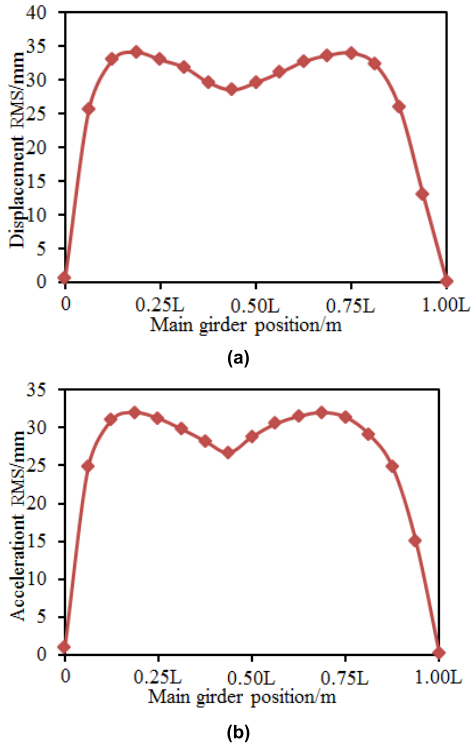

FIGURE 8. Vibration displacement and acceleration RMS at different positions of the bridge. (a) Vibration displacement. (b) Vibration acceleration.

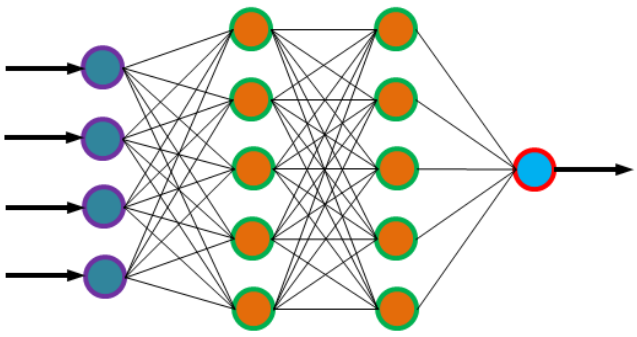

FIGURE 9. Topological structure of the neural network model.

introduced the ACO algorithm into optimization training of the BPNN model. A forward-feedback neural network training model based on the ACO algorithm (ACO-BPNN) was established, as shown in Fig. 10. The basic idea of the ACO-BP algorithm is that a certain weight value scope is searched roughly by the ACO algorithm; the weight obtained at this moment is taken as the initial weight value of BPNN model; in this manner, the defects of the BPNN model, including falling into local minimum, slow convergence and oscillation effects could be improved.

The process of realization of the ACO-BPNN algorithm proposed in the paper is shown in Fig. 11. Specific details of the process are given as follows. 1) According to equal segments, all the weight candidate points of BPNN model are listed, the equal information initial values are assigned to each candidate point, and a nerve cell threshold value is set as a constant. 2) Artificial ants are randomly distributed to each candidate point of the weight, and these ants randomly select

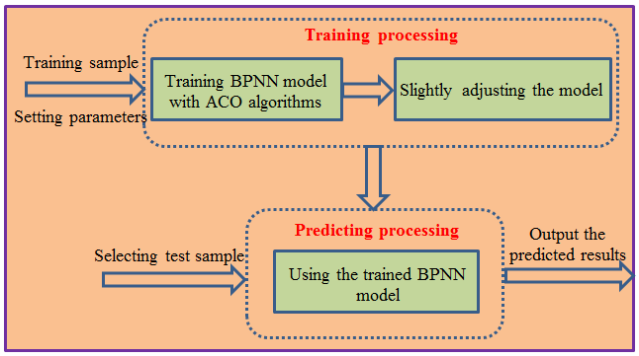

FIGURE 10. Construction of the proposed ACO-BPNN model.

a candidate point that does not pass the weight according to pheromones until completion of traversal of all the weights. It is assumed that M weights are going to be optimized. Each weight candidate point set is I. For ant m, the probability for it to select the j^{th} candidate point of the next weight is P. 3) All the weight combinations are recorded; they are input into the BPNN model. Learning samples and each network parameter are used to compute the network output deviation value corresponding to the combination. If the deviation value reaches a level that is slightly looser than the final neural network output required by the ACO algorithm, then the combination is taken as the optimal weight combination searched by the ant colony and assigned with the BPNN model; otherwise, the pheromone distribution is updated according to the deviation value, and the ant colony screening is repeated until the optimal combination is found or the ant colony iteration time reaches an upper limit. 4) The weight combination searched by the ant colony is taken as an initial value. The BPNN algorithm is used to learn samples repeatedly. Amendment of the weights and threshold values is continued until the final accuracy requirements are satisfied.

In this paper, a BPNN model with only one hidden layer was used to predict dynamic responses of the long-span bridge. The initial hidden layer node number was set to be 10. After the ACO algorithm was trained, it was found that performance of the neural network was not ideal. Thus, hidden layer nodes were added gradually. When the hidden layer node number increased to 20, the training was already conducted many times, the mean square errors were still large, and the performance of the neural network was still

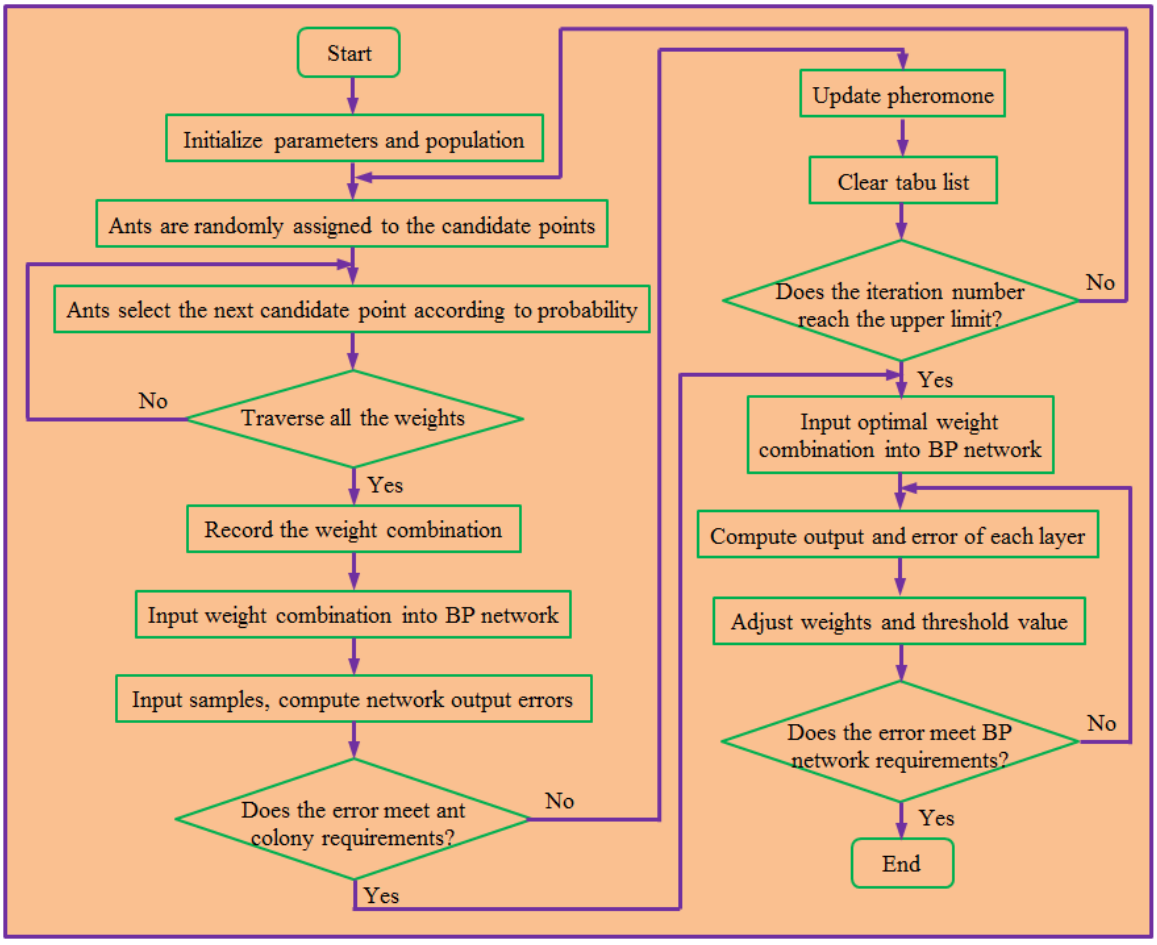

FIGURE 11. Flow chart of the improved BPNN model by the ant colony optimization algorithm.

TABLE 1. Training errors of three types of neural network models.

Three types of BPNN models	Number of iterations	Errors	Number of iterations	Errors
BPNN model	80	0.155	600	0.0026
GA-BPNN model	80	0.120	315	0.0095
ACO-BPNN model	80	0.055	130	0.0090

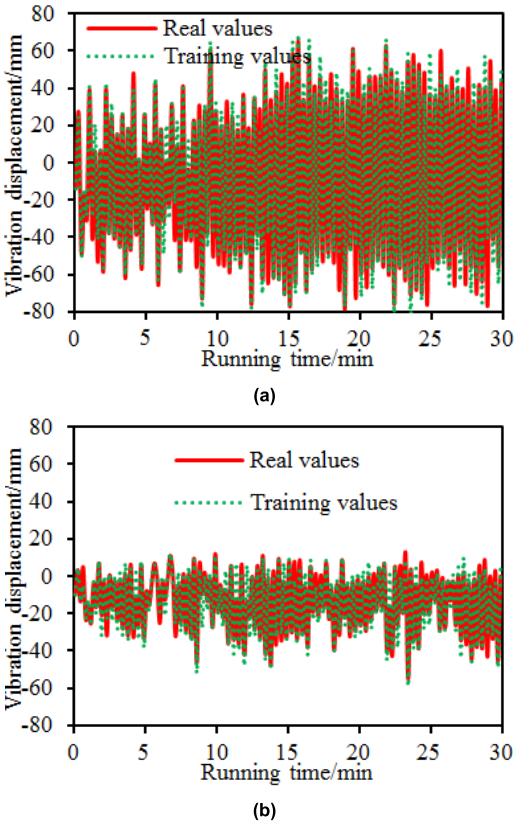

FIGURE 12. Training of the vibration displacement using the ACO-BPNN. (a) Position = L/4. (b) Position = L/2.

unsatisfactory. Therefore, the BPNN model with two hidden layers was used, as shown in Fig. 9. To determine the node number of the first hidden layer and that of the second hidden layer, the paper set the node number scope of the first hidden layer to be [5] and [15] and set the node number scope of the second hidden layer to be [1] and [5]. Next, the corresponding neural networks were established. The mean square error values of each neural network with the same training times were compared to select a relatively better neural network. To reduce the effects caused by randomness, under each case, the average value of 10 cycles was taken as the final value under the case. The critical error was 0.01. To further confirm the validity of the ACO-BPNN model after parameter selection, it was compared with the traditional BPNN model and the GA-BPNN model. BPNN, GA-BPNN and ACO-BPNN adopt the same network topology structure to predict dynamic responses of the long-span bridge. The training errors of the three types of models are shown in Table 1. The termination condition of the iteration

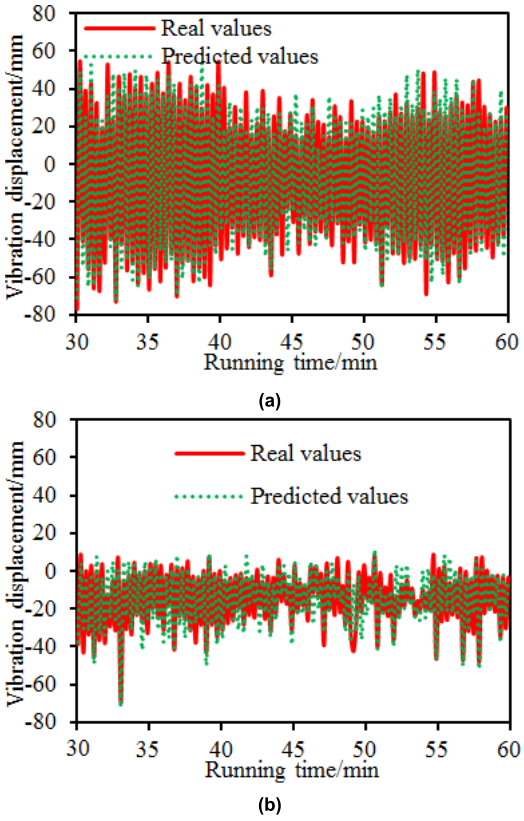

FIGURE 13. Predicted results of the vibration displacement using the ACO-BPNN. (a) Position = L/4. (b) Position = L/2.

of the three types of models is when the set iteration generation number reaches 600. It is shown in Table. 1 that the training errors were 0.155, 0.120 and 0.055 when the BPNN, GA-BPNN and ACO-BPNN models, respectively, conducted an iteration to the 80^{th} generation, where all the values exceeded the set critical error value. When the iteration was conducted to the 130^{th} generation, the training error of the ACO-BPNN model was 0.009, which is less than the set critical error value of 0.01. When the iteration was conducted to the 315^{th} generation, the GA-BPNN model achieved convergence, and the error was 0.0095 and less than the set critical error. When the iteration was conducted to the 600^{th} generation, the training error of the BPNN model was 0.0026, which is still larger than the critical error, and the model did not achieve convergence. When the ACO-BPNN model conducted the iteration to the 130^{th} generation, the training error was 0.009, which is less than the set critical error. In this manner, the computational accuracy was increased, and the optimized time was reduced.

The analysis above shows that the ACO-BPNN model proposed by the paper has prominent advantages; thus, the model was used to predict dynamic responses of the long-span bridge. First, the first 30 min of vibration displacement of the long-span bridge was extracted as the training data to train the ACO-BPNN model. The training data were compared with real data, as shown in Fig. 12. It is shown in

the figure that the training data and actual data could coincide well and that the peak and valley points were consistent. The result indicates that the ACO-BPNN model was well trained and had good performance. The last 30 min of data of the vibration displacement of the long-span bridge were taken as the predicted data. The trained ACO-BPNN model was used to predict the vibration displacement of the long-span bridge. The predicted results were compared with the actual values, as shown in Fig. 13. Fig. 13 shows that the predicted values and the actual values coincided well and that the peak and valley points were kept consistent. The result shows that the ACO-BPNN model proposed in this paper has high reliability in predicting dynamic responses of the long-span bridge. In addition, the proposed ACO-BPNN model only required 0.4 hours to predict the dynamic response of the long-span bridge. In the case of the same computer performance, the finite element required 4.5 hours to predict the dynamic response of the long-span bridge. The advantages of the proposed ACO-BPNN model in predicting the performance of large-scale complex structures such as a long-span bridge were clearly found.

V. CONCLUSIONS

1) The vibration shapes at the top 10 orders of the long-span bridge were extracted. The frequencies of each order of vibration shapes were 0.51 Hz, 0.67 Hz, 0.76 Hz, 0.85 Hz, 0.96 Hz, 1.06 Hz, 1.12 Hz, 1.21 Hz, 1.34 Hz and 1.56 Hz. Clearly, the observed very dense frequency distribution was found to satisfy the dense distribution characteristic of natural frequencies of large infrastructures. Vibration shapes of the long-span bridge were not found to be purely torsional or bending vibration; sometimes, they referred to overlaying of the two types of vibration.

2) The responses at different positions of the long-span bridge were found to be different. The displacement response peak value at the L/4 position was approximately 1.14 times compared with the displacement response peak at the L/2 position.

3) The experimental testing results showed that the numerical computation model proposed by the paper is reliable. Therefore, the root-mean-square values of the vibration displacements at each position of the bridge were computed based on the numerical model. The root-mean-square values of the bridge vibration displacement were basically symmetrical relative to the mid-span position. Within 0-L/4, the root-mean-square values of the vibration displacement sharply increased to the maximum value and then decreased slowly. The maximum root-mean-square values of the vibration displacement were approximately at the positions of L/4 and 3L/4 of the bridge. The valley values of the root-mean-square curve were located at the bridge mid-span position.

4) BPNN, GA-BPNN and ACO-BPNN adopted the same network topology structure to predict the dynamic responses of the long-span bridge. When the ACO-BPNN model conducted the iteration to the 130th generation, the training error of 0.009 was smaller than the set critical error. Only 0.4 hours were spent in using the proposed ACO-BPNN model to predict the dynamic response of the long-span bridge. In the case of the same computer performance, 4.5 hours were required for the finite element to predict the dynamic response of the long-span bridge. The advantages of the proposed ACO-BPNN model in predicting the performance of large-scale complex structures such as a long-span bridge were clearly found.

REFERENCES

[1] K. Cui, W.-H. Yang, and H.-Y. Gou, "Experimental research and finite element analysis on the dynamic characteristics of concrete steel bridges with multi-cracks," *J. Vibroeng.*, vol. 19, no. 6, pp. 4198–4209, Sep. 2017.
[2] K. H. Cho *et al.*, "Inspection robot for hanger cable of suspension bridge: Mechanism design and analysis," *IEEE/ASME Trans. Mechatronics*, vol. 18, no. 6, pp. 1665–1674, Dec. 2013.
[3] M. Domaneschi and L. Martinelli, "Performance comparison of passive control schemes for the numerically improved ASCE cable-stayed bridge model," *Earthquakes Struct.*, vol. 3, no. 2, pp. 181–201, Apr. 2012.
[4] M. Kurata *et al.*, "Internet-enabled wireless structural monitoring systems: Development and permanent deployment at the new Carquinez suspension bridge," *J. Struct. Eng.*, vol. 139, no. 10, pp. 1688–1702, Oct. 2013.
[5] M.-F. Liu, T.-P. Chang, and D.-Y. Zeng, "The interactive vibration behavior in a suspension bridge system under moving vehicle loads and vertical seismic excitations," *Appl. Math. Model.*, vol. 35, no. 1, pp. 398–411, Jan. 2011.
[6] S.-W. Kim and N.-S. Kim, "Dynamic characteristics of suspension bridge hanger cables using digital image processing," *NDT & E Int.*, vol. 59, pp. 25–33, Oct. 2013.
[7] D. Gąska, J. Margielewicz, T. Matyja, T. Haniszewski, T. Matyja, and P. Chróst, "Numerical identification of the overhead travelling crane's dynamic factor caused by lifting the load off the ground," *J. Meas. Eng.*, vol. 3, no. 1, pp. 1–8, Mar. 2015.
[8] J. Musayev, G. Abdugaliyeva, Z. Yessenkluova, A. Zhauyt, G. Mamatova, and T. Buzauova, "The experimental determination of the stress calculation and relative strains in the span elements of railway bridges under the influence of the rolling equipment," *J. Meas. Eng.*, vol. 5, no. 3, pp. 125–133, May 2017.
[9] Y. L. Xu, Q. Lia, D. J. Wu, and Z. W. Chen, "Stress and acceleration analysis of coupled vehicle and long-span bridge systems using the mode superposition method," *Eng. Struct.*, vol. 32, no. 5, pp. 1356–1368, May 2010.
[10] H. Wang, A.-Q. Li, and J. Li, "Progressive finite element model calibration of a long-span suspension bridge based on ambient vibration and static measurements," *Eng. Struct.*, vol. 32, no. 9, pp. 2546–2556, Sep. 2010.
[11] X. Kong, D. J. Wu, C. S. Cai, and Y. Q. Liu, "New strategy of substructure method to model long-span hybrid cable-stayed bridges under vehicle-induced vibration," *Eng. Struct.*, vol. 34, pp. 421–435, Jan. 2012.
[12] N.-H. Ding, Y.-J. Qian, L.-X. Lin, and Y.-P. Wu, "Vibration character of a double cable suspension bridge under a single vehicle load," *J. Vibrat. Shock*, vol. 29, no. 7, pp. 216–220, Apr. 2010.
[13] H. P. Pang, J. G. Wang, and F. Qian, "Analysis of vehicle-bridge interaction of long span suspension bridges," *J. Hefei Univ. Technol.*, vol. 34, no. 1, pp. 114–118, Jan. 2011.
[14] X. Xiao and W. X. Ren, "The modeling and vibration analysis of the train-bridge interaction for a long span railway bridge with four line," *J. Vibrat. Eng.*, vol. 27, no. 4, pp. 497–506, Aug. 2014.
[15] Y. Shi, Y.-F. Song, H. Sun, and X.-P. Zhou, "Dynamic analysis method of vehicle-bridge coupling for complicated bridges based on ANSYS," *J. Tianjin Univ.*, vol. 43, no. 6, pp. 537–543, Jun. 2010.
[16] M. Ye, P. Zhang, J. Y. Fu, W. B. Cao, and M. Ren, "Coupled vehicle-bridge evolutionary random vibration for a multi-span continuous bridge with elastic bearings," *J. Vibrat. Shock*, vol. 33, no. 3, pp. 76–82, Feb. 2014.
[17] X. Zhang, D. Du, Y. Chai, and J.-Q. Liu, "Analysis of influences of different factors on continuous rigid frame bridges based on theory of vehicle-bridge system coupling vibration," *J. Central South Univ., Sci. Technol.*, vol. 47, no. 8, pp. 2848–2854, Aug. 2016.
[18] J. B. Zhang, J. B. Liao, G. W. Tang, and W. T. Xu, "Dynamic response of a bridge considering its surface random unevenness," *J. Vibrat. Shock*, vol. 35, no. 7, pp. 214–219, Apr. 2016.

[19] M. Ye, P. Tan, M. Ren, F. L. Zhou, and X. L. Ning, "Evolutionary random vibration analysis of a bridge subjected to moving vehicles," *J. Vibrat. Eng.*, vol. 23, no. 3, pp. 269–274, Mar. 2010.

[20] B. H. Ji *et al.*, "Research on stress spectrum of steel decks in suspension bridge considering measured traffic flow," *J. Perform. Constructed Facilities*, vol. 26, no. 1, pp. 65–75, Feb. 2012.

[21] J. Wu and S. D. Blostein, "High-rate diversity across time and frequency using linear dispersion," *IEEE Trans. Commun.*, vol. 56, no. 9, pp. 1469–1477, Sep. 2008.

[22] S. P. Carroll, J. S. Owen, and M. F. M. Hussein, "A coupled biomechanical/discrete element crowd model of crowd–bridge dynamic interaction and application to the Clifton Suspension Bridge," *Eng. Struct.*, vol. 49, pp. 58–75, Apr. 2013.

[23] J. M. Rocha, A. A. Henriques, and R. Calçada, "Safety assessment of a short span railway bridge for high-speed traffic using simulation techniques," *Eng. Struct.*, vol. 40, pp. 141–154, Jul. 2012.

[24] Z.-H. Zong, F.-F. Li, W.-W. Yuan, and Y.-F. Xia, "Study of vehicle load models for Xinyi river bridge based on WIM data," *Bridge Construction*, vol. 43, no. 5, pp. 29–36, Dec. 2013.

[25] T. Yoshino, Y. Sano, D. Ota, K. Fujita, and T. Ikui, "Fiber-Bragg-grating based single axial mode Fabry–Pérot interferometer and its strain and acceleration sensing applications," *J. Lightw. Technol.*, vol. 34, no. 9, pp. 2241–2250, May 1, 2016.

[26] P. Xiao, J. Wu, and C. F. N. Cowan, "MIMO detection schemes with interference and noise estimation enhancement," *IEEE Trans. Commun.*, vol. 59, no. 1, pp. 26–32, Jan. 2010.

[27] M. Kim, J.-H. Jeong, H. Kim, and D. Gweon, "A six-degree-of-freedom magnetic levitation fine stage for a high-precision and high-acceleration dual-servo stage," *Smart Mater. Struct.*, vol. 24, no. 10, pp. 1–8, Sep. 2015.

[28] J.-Q. Li, S.-Q. He, S. Cai, and Z. Ming, "An intelligent wireless sensor networks system with multiple servers communication," *Int. J. Distrib. Sensor Netw.*, vol. 11, no. 8, pp. 1–9, Aug. 2015.

[29] J. Du, P. Xiao, J. Wu, and Q. Chen, "Design of isotropic orthogonal transform algorithm-based multicarrier systems with blind channel estimation," *IET Commun.*, vol. 6, no. 16, pp. 2695–2704, Nov. 2012.

[30] H. Koch, A. Konig, A. Weigl-Seitz, K. Kleinmann, and J. Suchy, "Multisensor contour following with vision, force, and acceleration sensors for an industrial robot," *IEEE Trans. Instrum. Meas.*, vol. 62, no. 2, pp. 268–280, Feb. 2012.

[31] W. Wei *et al.*, "Gradient-driven parking navigation using a continuous information potential field based on wireless sensor network," *Inf. Sci.*, vol. 408, pp. 100–114, Oct. 2017.

[32] T. Wang, H. Gao, and J. Qiu, "A combined adaptive neural network and nonlinear model predictive control for multirate networked industrial process control," *IEEE Trans. Neural Netw. Learn. Syst.*, vol. 27, no. 2, pp. 416–425, Feb. 2015.

[33] J.-Q. Li, L. Huang, S. He, Z. Ming, and Y. Zhou, "Computation partitioning for mobile cloud computing in a big data environment," *IEEE Trans. Ind. Informat.*, vol. 13, no. 4, pp. 2009–2018, Aug. 2017.

[34] K. Cui and T. T. Zhao, "Unsaturated dynamic constitutive model under cyclic loading," *Cluster Comput.*, vol. 20, no. 4, pp. 2869–2879, 2017.

[35] M. Valipour, M. E. Banihabib, and S. M. R. Behbahani, "Comparison of the ARMA, ARIMA, and the autoregressive artificial neural network models in forecasting the monthly inflow of Dez dam reservoir," *J. Hydrol.*, vol. 476, pp. 433–441, Jan. 2013.

[36] A. Yang *et al.*, "Optimum surface roughness prediction for titanium alloy by adopting response surface methodology," *Results Phys.*, vol. 7, pp. 1046–1050, 2017.

[37] K. Cui and X. Qin, "Virtual reality research of the dynamic characteristics of soft soil under metro vibration loads based on BP neural networks," *Neural Comput. Appl.*, vol. 29, no. 5, pp. 1233–1242, Mar. 2018.

LIWEN ZHANG received the B.S. and M.S. degrees in civil engineering from Guangzhou University, Guangzhou, China, in 2005 and 2008, respectively, and the Ph.D. degree in bridge engineering from Tongji University, Shanghai, China, in 2014. He is currently a Lecturer with the Department of Civil Engineering, Guangzhou University. His current research interests include test, detection and assessment of bridge structure, and new material application.

ZHUO SUN received the B.S. degree in railway engineering and the M.S. and Ph.D. degrees in bridge and tunnel engineering from Beijing Jiaotong University, Beijing, China, in 1995, 1998, and 2002, respectively. He is currently an Associate Professor with the Department of Civil Engineering, Guangzhou University. His current research interests include test, detection and assessment of bridge structure, and seismic engineering.

CHAO ZHANG received the B.S. and M.S. degrees in civil engineering from Guangzhou University, Guangzhou, China, in 2005 and 2008, respectively, and the Ph.D. degree in civil engineering from Tongji University, Shanghai, China, in 2014. He is currently An Associate Professor with the Department of Civil Engineering, Guangzhou University. His current research interests include seismic reduction and isolation of structure, and new material application.

FENGHUI DONG received the B.S. degree in civil engineering from the Nanjing University of Aeronautics and Astronautics, Nanjing, China, in 2010, and the M.S. degree in bridge and tunnel engineering from Chang'an University, Xi'an China, in 2013. He is currently pursuing the Ph.D. degree in bridge engineering with Tongji University, Shanghai, China. His current research interests include wind resistance theory of long-span bridges, dynamic analysis of long-span structure, risk and reliability theory of structures, and analysis and design theory of long-span bridges.

PU WEI received the B.S. and Ph.D. degrees in civil engineering from Tongji University, Shanghai, China, in 2009 and 2015, respectively. He is currently a Senior Engineer with the Shanghai Municipal Engineering Design Institute, Shanghai, China. His current research interests include bridge design and assessment.